Engineering Microbiology 4 (2024) 100176

Contents lists available at ScienceDirect

Engineering Microbiology

journal homepage: www.elsevier.com/locate/engmic

Original Research Article

Immobilization of *Thermomyces lanuginosus* lipase on metal-organic frameworks and investigation of their catalytic properties and stability

Zeynab Rangraz[a], Mostafa M. Amini[b], Zohreh Habibi[a,*]

[a] Department of Organic Chemistry, Faculty of Chemistry, Shahid Beheshti University, G.C., Tehran, Iran
[b] Department of Inorganic Chemistry, Faculty of Chemistry, Shahid Beheshti University, G.C., Tehran, Iran

ARTICLE INFO

Keywords:
Biocatalyst
MOF
Enzyme immobilization
Lipase
Thiazoles

ABSTRACT

Surface adsorption is a convenient and readily available method for immobilizing enzymes on metal-organic frameworks (MOFs). Metal-organic framework-5 (MOF-5), isoreticular metal-organic frameworks-3 (IRMOF-3), and multivariate analysis of MOF-5/IRMOF-3 (MMI) with a half-amino group (-NH_2) were prepared in this study. *Thermomyces lanuginosus* lipase (TLL) was chosen as a commercially available enzyme for immobilization on the surfaces of these MOFs. Briefly, 1.5 mg of TLL was added to 10 mg of the MOFs, and after 24 h, 67, 74, and 88% of the TLL was immobilized on MOF-5, IRMOF-3, and MMI, respectively. Fourier transform infrared spectroscopy, X-ray diffraction, thermogravimetric analysis, scanning electron microscopy, energy-dispersive X-ray analysis, and Brunauer–Emmett–Teller analysis were used to characterize the resulting biocomposites. TLL@MOF-5, TLL@IRMOF-3, and TLL@MMI exhibited activities of 55, 75, and 110 U/mg, respectively. Investigation of the activity and stability of the prepared biocatalysts showed that TLL immobilized on MMI was 2.34-fold more active than free TLL. TLL@MMI exhibited high stability and activity even under harsh conditions. After 24 h of incubation in a mixture of 50% (v/v) MeOH, TLL@MMI retained 80% of its activity, whereas TLL@MOF-5 and free TLL lost 50 and 60% of their activities, respectively. TLL@MMI was used to synthesize 2-arylidenehydrazinyl-4-arylthiozole derivatives (91–98%) in a one-pot vessel by adding benzaldehydes, phenacyl bromides, and thiosemicarbazide to water. The efficiency of the 4a derivative with free TLL was 43%, whereas that with TLL@MMI was 98%.

1. Introduction

Enzymes are used in various industries and have great potential for further applications. However, harsh conditions, such as high temperatures, non-aqueous solvents, high salt concentrations, and extreme pH, negatively affect the structure and activity of the enzyme [1–5]. Other disadvantages of this enzyme include the high cost of purification, isolation, and non-reusability. Various methods have been proposed to overcome these limitations. One of the most effective methods is enzyme immobilization. Enzyme immobilization not only solves these problems but can also increase enzyme stability. The structure of the enzyme may change after immobilization. These changes can decrease enzymatic activity, an inherent disadvantage of enzyme immobilization [6–9].

Lipases (triacylglycerol hydrolases, EC 3.1.1.3) catalyze numerous reactions, such as esterification [10], transesterification [11], alcoholysis [12], and hydrazinolysis [13]. Lipases are popular catalysts in the chemical industry and academia for several reasons. First, these enzymes work in non-aqueous conditions. Second, they do not require cofactors to perform the reactions. Third, they show high substrate tolerance. Despite these advantages, however, they also have some disadvantages, such as the difficulty separating them from the reaction medium and the subsequent inability to recover them, increasing costs [14–18].

Lipase immobilization on porous materials such as silica, sol-gel matrices, hydrogels, and organic microparticles has been studied for decades [19,20]. Metal-organic frameworks (MOFs) are a new group of porous materials made from metal ions and organic compounds linked through coordination bonds. Owing to their porous structure, large surface area, and thermal and chemical stability, MOFs have received increasing attention for enzyme immobilization applications [21,22]. Enzyme immobilization on MOFs can be categorized into four main types: surface attachment, covalent linkage, pore entrapment, and coprecipitation. During surface attachment, the enzyme attaches to the MOF via physical interactions. These weak interactions include hydrogen bonding, van der Waals interactions, and π-π interactions [23]. Enzyme immobilization onto MOF surfaces is the most straightforward method, as enzymes bind through weak interactions, and activating the functional groups is unnecessary. This method makes it possible for the MOF to be synthesized separately, and its synthetic conditions would not affect

* Corresponding author.
E-mail address: z_habibi@sbu.ac.ir (Z. Habibi).

https://doi.org/10.1016/j.engmic.2024.100176
Received 13 June 2024; Received in revised form 20 October 2024; Accepted 21 October 2024
Available online 28 October 2024

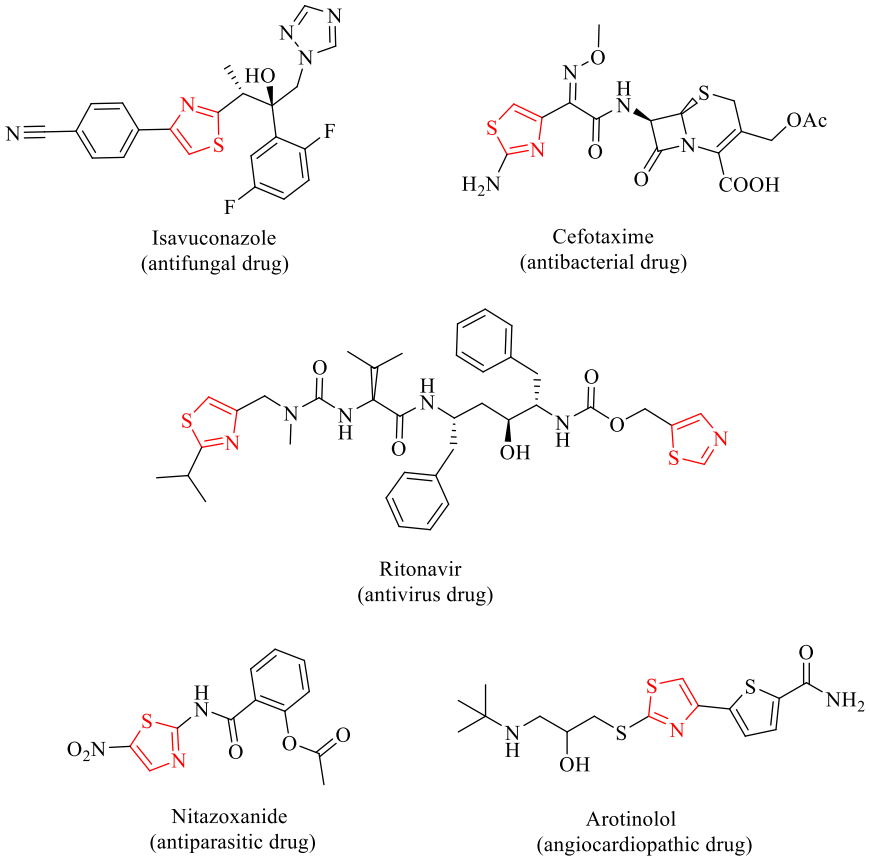

Fig. 1. Some examples of drugs containing thiazoles.

enzyme activity; therefore, a wide range of MOFs can be used as carriers [24,25].

Maintaining the structure of an enzyme and its active sites is one of the positive features of enzyme adsorption onto MOF surfaces. However, compared to other immobilization methods, this method gives the enzyme less stability and resistance to harsh conditions, such as organic solvents and high temperatures [26]. Therefore, modifying MOFs with amino groups overcomes this problem.

Lipases have lids consisting of hydrophobic polypeptide chains. This lid opens in the presence of a hydrophobic agent, thereby exposing the active site and the hydrophobic pocket. Lipases can be adsorbed onto a hydrophobic surface through a hydrophobic pocket through a process called interface activation. Hence, lipases can be immobilized on a hydrophobic substrate with an open lid to maintain their activity [27–29]. In recent years, stable hydrophobic MOFs have been prepared using organic bonds or post-synthetic modifications with hydrophobic groups or materials. ZIF-8, ZIF-L, ZIFN, and Uio-66-NH_2-OA are examples of MOFs successfully used to immobilize lipases via surface adsorption [23,30].

Lipase from *Thermomyces lanuginosus* (TLL) is an *sn*-1,3-specific lipase widely used for the synthesis of organic compounds and biodiesel production. The immobilization of TLL has been the subject of many studies [27,31]. Carriers such as amine-functionalized magnetic nanoparticles, multi-walled carbon nanotubes, and magnetic macroporous zeolitic imidazolate framework-8 (m-M-ZIF-8) have been used to immobilize TLL through covalent bond formation or physical adsorption. Previous investigations showed that the catalytic properties of TLL, such as enzyme activity, organic solvent tolerance, and reusability, significantly improved after immobilization [19,32,33].

Compounds containing five aromatic rings with nitrogen and sulfur groups are called thiazoles. This heterocyclic structure has various biological properties, such as antimicrobial, antineoplastic, antiretroviral, and antifungal [34,35]. Thiazoles are part of the structure of many drugs, such as savuconazole, cefotaxime, ritonavir, nitazoxanide, and atrotinolol (Fig. 1) [35]. Owing to their importance, various catalysts have been used to synthesize these scaffolds, as shown in Table 1. The disadvantages of these methods include harsh reaction conditions, the need to separate the intermediates, and the use of toxic solvents. Therefore, efficient, cost-effective, and recyclable catalysts are required to synthesize them.

In addition to their natural catalytic role, lipases can also catalyze other reactions, such as the Michael addition [36–38], Mannich [39], Ugi [40], Cannizaro [41], and Baylis–Hilman [42] reactions. This characteristic of lipases is called promiscuity and has received considerable attention [43]. In this study, this lipase was used to synthesize thiazole derivatives.

Accordingly, for the first time, three MOFs, MOF-5, isoreticular metal-organic framework-3 (IRMOF-3), and multivariate analysis of MOF-5/IRMOF-3 (MMI) with a half-amino group (-NH_2) were used to immobilize TLL and generate three biocomposites: TLL@MOF-5, TLL@IRMOF-3, and TLL@MMI. The effects of pH, solvent, and temperature on the stability of the three biocomposites were investigated. Moreover, because of the increasing interest in green methods for the synthesis of organic compounds, the prepared biocatalysts were used to synthesize thiazoles. Since thiazole is widely used in various drugs, its synthesis using a green method is important.

2. Materials and Methods

2.1. Materials

TLL and phenacyl bromide were purchased from Sigma-Aldrich (St. Louis, MO, USA). Zinc nitrate tetrahydrate ($Zn(NO_3)_2{\cdot}4H_2O$), terephthalic acid (H_2BDC), 2-aminoterephthalic acid, aldehydes, thiosemicarbazide, and other chemicals were purchased from Merck. The structures of the thiazoles were characterized using ^1H (300 MHz) and ^{13}C (75 MHz) nuclear magnetic resonance (NMR) using a Bruker NMR spec-

Table 1
Reaction parameters previously reported for synthesizing compound 4a.

Entry	Compound	Reagent/Catalyst (condition)	One-pot	Yield (%)	Ref.
1	4a	$NaHCO_3/K_2CO_3$ (reflux)	No	72	[74]
2	4a	AcOH (reflux)	No	61	[72]
3	4a	TCCA[1]/*p*-TSA[2] K_2CO_3 (ball-milling)	Yes	84	[75]
4	4a	a few drops of DMF	No	82	[76]
5	4a	CuONPs/TiO_2[3] (RT)	Yes	98	[73]

[1] trichloroisocyanuric acid
[2] p- toluenesulfonic acid
[3] copper nanoparticles supported on TiO_2

trometer. Dimethyl sulfoxide-d_6 (DMSO-d_6) was purchased from Mesbah Energy Co., Ltd..

2.2. MOF characterization

Scanning electron microscopy (SEM; SU3500) was used to determine the surface morphology of the MOFs. The constituent elements of TLL and TLL@MMI were analyzed using energy-dispersive X-ray (EDX) in conjunction with SEM. MOF-5, MMI, and IRMOF-3 were subjected to X-ray diffraction (XRD) using a scintillation counter with Cu radiation (λ=1.5406 Å). Thermogravimetric analysis (TGA) was performed using a thermogravimetric analyzer (STAPT 1600) in an air environment from 25 ˚C to 600 ˚C, increasing at a rate of 20 ˚C/min. Fourier transform infrared spectroscopy (FT-IR) was conducted using a Bruker Equinox 55 system within the wavenumber range of 600–3800 cm^{-1}. The percentages of carbon, nitrogen, and hydrogen in IRMOF-3 and MMI were determined using an Elementar Analysensysteme GmbH device. Meanwhile, a Brunauer–Emmett–Teller (BET) Surface Area & Porosity Analyzer (BET), BELSORP Mini II) was used to determine the surface areas of the MOFs and TLL@MOFs.

2.3. Preparation of MOFs

MOF-5 was prepared using the solvothermal method with some modifications, as reported in the literature [44]. In detail, 0.553 g H_2BDC and 2.61 g $Zn(NO_3)_2{\cdot}4H_2O$ were added to 87 ml *N,N*-dimethylformamide (DMF) and stirred for 10 minutes at 25 ˚Cuntil a clear solution was obtained, and then the solution was transferred to a Teflon reactor and kept at 105 ˚C for 21 h. Subsequently, the reaction mixture was cooled to room temperature, and the product was separated via centrifugation. The product was then washed twice with DMF, and the colorless crystals were soaked in MeOH for approximately 7 days. The MeOH was changed every other day. Afterward, the crystals were separated from the MeOH and dried in an oven for 3 h at 100˚C.

MTV-MOF-5/IRMOF-3 (MMI), which contains a mixture of 2-aminoterephthalic acid and H_2BDC instead of a full 2-aminoterephthalic acid ligand in their structure, was synthesized using the solvothermal method [45,46]. Briefly, 0.137 g 2-aminoterephthalic acid, 0.208 g H_2BDC, and 1.56 g $Zn(NO_3)_2{\cdot}4H_2O$ were dissolved in 75 ml DMF, then transferred to a Teflon reactor and kept at 105 ˚C for 21 h. Finally, the obtained crystals were activated in a manner similar to MOF-5 synthesis.

IRMOF-3 was synthesized by dissolving 0.48 g $Zn(NO_3)_2{\cdot}4H_2O$ and 0.12 g 2-aminoterephthalic acid in 15 ml DMF, transferring the mixture to a Teflon reactor and keeping it at 105 ˚C for 21 h. Finally, the obtained crystal was activated in a manner similar to MOF-5 synthesis [47].

2.4. Preparation of TLL@MOFs

All TLL@MOFs were prepared by adding 1.5 mg (100 µl) of TLL (16 mg/ml) to 10 mg MOF and stirred at 200 rpm for 24 h at 15–20 ˚C. The resulting biocomposite was centrifuged and washed three times with potassium phosphate buffer (pH 7.2) and dried with a vacuum system at 25 ˚C for 2–3 h.

2.5. Determining the amount of enzyme immobilized on the MOFs

The percentage of immobilized enzymes on the MOFs was calculated using the Bradford method [48]. The difference between the amount of enzyme remaining after immobilization and the initial enzyme concentration was determined as the immobilization percentage. To ensure the accurate calculation of the immobilization yield and that the immobilized enzyme did not separate from the hydrophobic substrate during washing [49], the enzyme concentration in the biocomposite washing buffer was also calculated using the Bradford method. TLL@MMI and TL@IRMOF-3 did not release the enzyme, whereas approximately 1% of the enzyme was released by TLL@MOF-5; these were ignored in the calculations.

2.6. Activity assay of free and immobilized TLL

The activities of the free and immobilized enzymes were assessed by calculating the amount of *p*-nitrophenol produced during *p*-nitrophenyl butyrate (*p*-NPB) hydrolysis in 10 mM potassium phosphate buffer at pH 8.2 and 25 ˚C. At the beginning of the reaction, 20 µl of the enzyme suspension (2 mg immobilized enzyme in 20 ml of 10 mM phosphate buffer [pH 7.2]) was added to 2 ml of the reaction mixture (20 µl of 30 mM *p*-NPB in 10 mM potassium phosphate buffer [pH 8.2]). Afterward, the absorbance change at 410 nm (ε = 17500 M^{-1} cm^{-1}) was measured over 2 min. Finally, the specific activity (U/mg) was calculated from the amount of immobilized enzyme. Meanwhile, 20 µl of TLL was dissolved in 10 ml of 10 mM potassium phosphate buffer [pH 7.2] to measure the activity of the free enzyme using the *p*-NPB assay. To confirm the lack of catalytic activity of MOFs with *p*-NPB, their activities were measured using the *p*-NPB assay, confirming that *p*-NPB was not hydrolyzed by the MOFs.

2.7. Leaching test

Briefly, 3 mg of TLL@MOF was added to solutions containing 1 M NaCl, and the mixture was incubated for 24 h. The enzyme concentration in the mixture was measured using the Bradford method.

2.8. Determination of pH stability and the pH with optimum enzyme activity

To determine the best pH where the enzyme has optimal stability, the free and immobilized enzymes were incubated in potassium phosphate buffer at different pH levels (6.5–10) for 24 h, and their activities were measured using the *p*-NPB assay. To determine the optimum pH, enzyme activities were measured using the *p*-NPB assay at different pH levels (6.5 to 10).

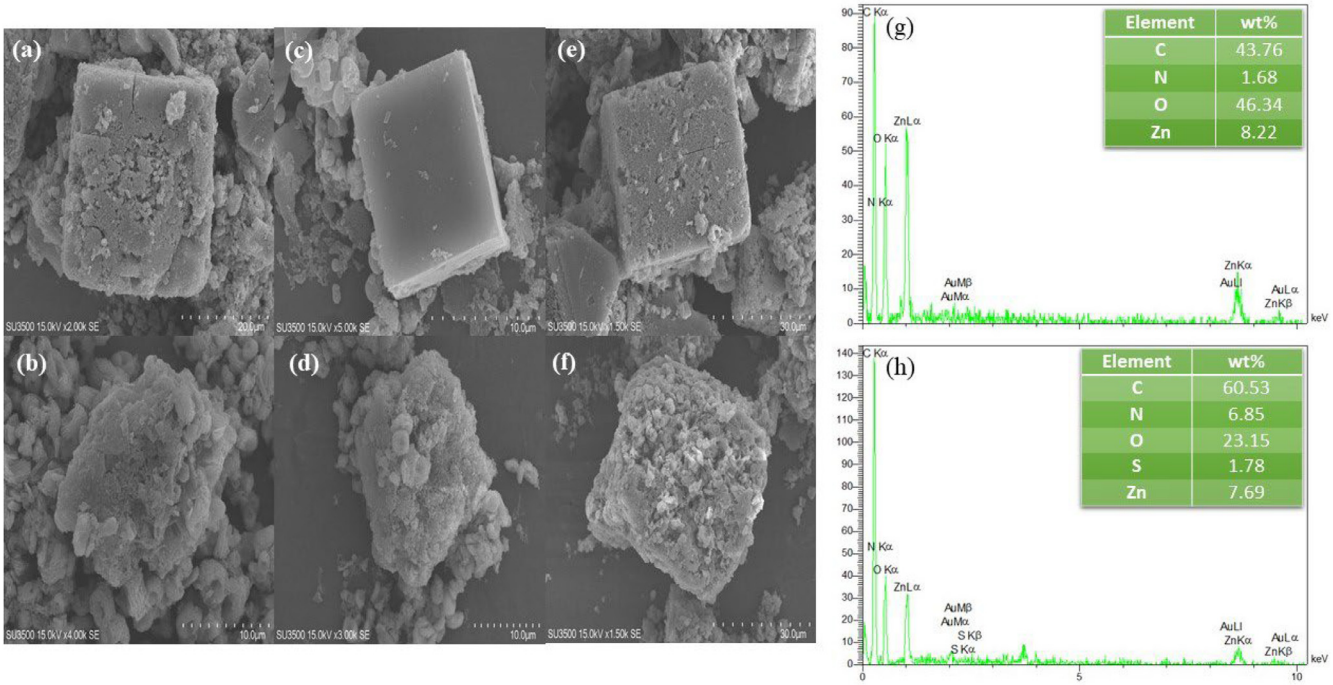

Fig. 2. Scanning electron microscopy images of the surfaces of a) MOF-5, b) TLL@MOF-5, c) IRMOF-3, d) TLL@IRMOF-3, e) MMI, and f) TLL@MMI. Energy-dispersive X-ray analyses of g) MMI and h) TLL@MMI.

2.9. Thermal stability

To measure the thermal stability of the immobilized enzymes, free and immobilized enzymes were incubated in potassium phosphate buffer at the pH with the optimal enzyme activity and subjected to different temperatures, at 45–85 °C for 2 h and at 45, 55, and 65 °C during 24 h. Enzymatic activity was measured using the *p*-NPB assay to determine the thermal stability of the enzyme.

2.10. Stability in organic co-solvents

To determine the stability of the TLL@MOFs in organic solvents, free and immobilized enzymes were incubated in 1 ml of a solution containing 10 mM potassium phosphate buffer (pH 7.2), 20% and 50% (v/v) MeOH, EtOH, THF, MeCN, DMF, and 1,4-dioxane at room temperature.

2.11. Synthesis of thiazoles

Thiazole was enzymatically synthesized in glass bottles containing 20 ml of a reaction mixture comprising 5 mmol aldehyde, 5 mmol acetophenone, and 5 mmol thiosemicarbazide dissolved in H_2O. The mixture was stirred at 200 rpm for 90 min at 45 °C with 10 mg of TLL@MMI. To purify the products, ethyl acetate (EtOAc) was added to obtain two phases, after which the aqueous phase was centrifuged to remove the catalyst. The EtOAc phase was then dried under vacuum. The obtained precipitate was washed twice with EtOAc to obtain the pure product.

2.12. Reusability of the TLL@MOFs

The catalyst used during thiazole synthesis was isolated to determine the number of times it could be used. After each reaction, the mixture was decanted with ethyl acetate, and the aqueous phase was centrifuged to separate the catalyst. The recovered catalyst was washed three times with potassium buffer (pH 9) and ethanol and then dried under vacuum for reuse. The activity of the recovered catalyst was measured using a *p*-NPB assay before being reused in subsequent reactions. All steps were repeated six times.

3. Results and Discussion

3.1. Characterization of MOFs and TLL@MOFs

The exterior structures of MOF-5, TLL@MOF-5, MMI, TLL@MMI, IRMOF-3, and TLL@IRMOF-3 are shown in (Fig. 2a–2f). The appearance of the TLL@MOFs indicated that the enzyme was coated onto the structure of the MOFs. The SEM images of MOF-5, MMI, and IRMOF-3 show a cubic shape, which is the typical morphology of each MOF. EDX is an X-ray technique used to detect the elemental or chemical properties of compounds [50]. EDX analysis was performed to confirm the addition of the enzyme. TLL contained Zn, C, N, and O (Fig. 2g), while the appearance of S in the EDX spectrum of TLL@MMI indicated the presence of the enzyme (Fig. 2h). Moreover, the nitrogen-to-zinc ratio is 0.2 and 0.9 in TLL and ILL@MMI, respectively. This increase in the amount of nitrogen confirms the presence of the enzyme in TLL@MMI.

XRD analysis provides detailed information on the crystallographic structure, chemical composition, and physical properties of materials [51]. The XRD patterns of MOF-5, IRMOF-3, and MMI are shown in Fig. 3. Strong diffraction peaks observed at 2θ values of 6.6°, 9.4°, and 13.5° are consistent with previous reports [45,46].

FT-IR involves the vibration and rotation of molecules at specific wavelengths [52]. These vibrations and rotations help elucidate the interactions between the enzyme and the MOF. The structures of MOF-5, TLL@MOF-5, IRMOF-3, TLL@IRMOF-3, MMI, and TLL@MMI were illustrated by FT-IR (Fig. 4a–4c). The peaks at wavenumbers 1606–1505 cm^{-1} and 1400–1256 cm^{-1} correspond to the BDC vibrations. The peaks at 1200–600 cm^{-1} can be attributed to the fingerprint of terephthalate [53]. The intensity of OH peaks related to the enzyme decreased after immobilization, which indicates the formation of hydrogen bonds [54,55].

The temperature resistance of biocomposites is an important issue. Thermogravimetric analysis (TGA) is a technique to evaluate the thermal resistance of materials [56]. The TGA results for MMI and TLL@MMI are shown in Fig. 4d. MMI showed high thermal stability up to 450 °C, then it lost 45% of its weight at temperatures up to 500

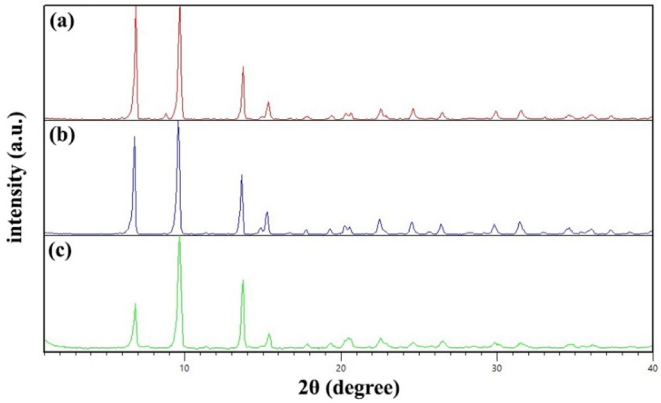

Fig. 3. X-ray diffraction patterns of a) MOF-5, b) MMI, and c) IRMOF-3.

˚C. TLL@MMI lost approximately 6% of its weight up at temperatures up to 150 ˚C; then, it lost 60% of its weight from 250 to 500 ˚C. Due to the presence of the enzyme on the MOF surface, the thermal resistance of the biocatalyst decreased. However, despite all these conditions, it is still stable up to 150 ˚C.

BET analysis is an approach to measure the specific surface area of a material [57]. The nitrogen adsorption-desorption isotherms of MOF-5, IRMOF-3, MMI, TLL@MOF-5, TLL@IRMOF-3, and TLL@MMI are shown in Fig. 5. According to these isotherms, the surface areas of MOF-5, IRMOF-3, and MMI are 445, 448, and 461 m^2/g, respectively. After immobilizing TLL on these supports, the surface areas were reduced to 104, 180, and 175 m^2/g, respectively. This decrease in the MOF surface area indicated the presence of enzymes.

CHN analysis was also performed to determine the number of amino groups in IRMOF-3 and MMI. For IRMOF-3, the amounts of carbon, hydrogen, and nitrogen were calculated to be 35.11%, 2.58%, and 5.12%, respectively, and the obtained values were 34.51% C, 2.6% H, and 5.21% N. Based on these calculations, MMI had 36.04% C, 2.65% H, and 2.63% N, and the obtained values were 35.89% C, 2.48% H, and 2.7% N.

3.2. Optimization of TLL@MOF preparation

To obtain the best activity and immobilization yield, the temperature, amount of enzyme, and stirrer rotation speed (rpm) were optimized. Initially, different amounts of the enzyme (Fig. 6a) were loaded on the carrier, and then 50–200 µl of free TLL was loaded on 10 mg of the substrate, and the highest enzyme activity was obtained using 100 µl of the enzyme. Subsequently, the stirrer rotation speeds were changed to 150, 200, 250, and 300 rpm; the optimal magnetic rotation speed was 200 rpm. The results showed that enzyme activity and immobilization yield decreased when the stirrer rotation speed increased. Moreover, the immobilization yield was also low when the stirrer rotation speed was lower than 200 rpm. The reaction system was also subjected to various temperatures (15–35 ˚C) to achieve the best results. The results showed that as the temperature increased, the immobilization yield also increased (Fig. 6b). For TLL@MMI, the immobilization yields were 98, 95, 90, 88, and 88% at temperatures of 35, 30, 25, 20, and 15 ˚C, respectively, with specific enzyme activities at 98, 100, 105, 110, and 110 U/mg, respectively. Our results suggest that enzyme activity decreased with increasing temperature, even though immobilization

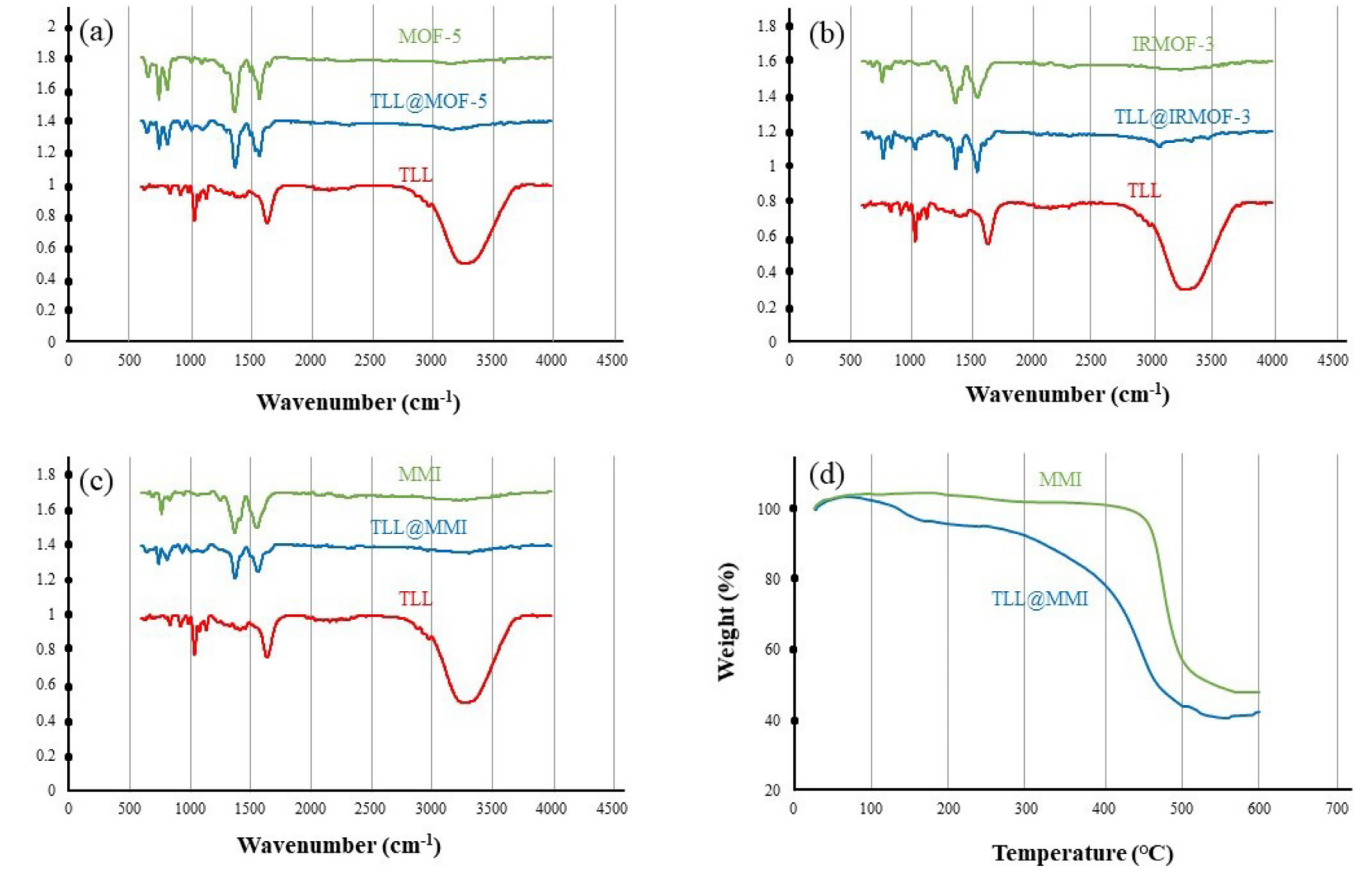

Fig. 4. Fourier transform infrared spectra of MOF-5, TLL@MOF-5 (a), IRMOF-3, TLL@IRMOF-3 (b), MMI, and TLL@MMI (c). TGA curves of MMI and TLL@MMI (d).

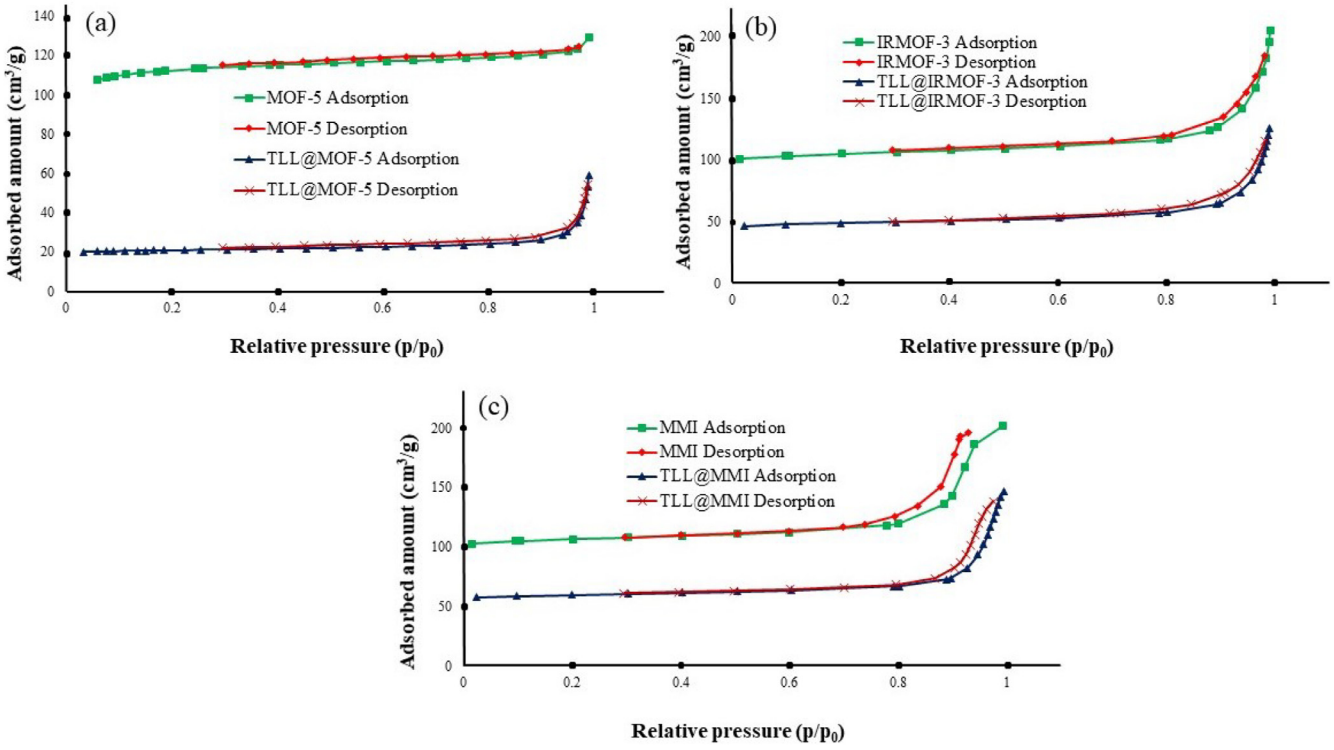

Fig. 5. Nitrogen adsorption-desorption isotherms of a) MOF-5 and TLL@MOF-5, b) IRMOF-3 and TLL@IRMOF-3, and c) MMI and TLL@MMI.

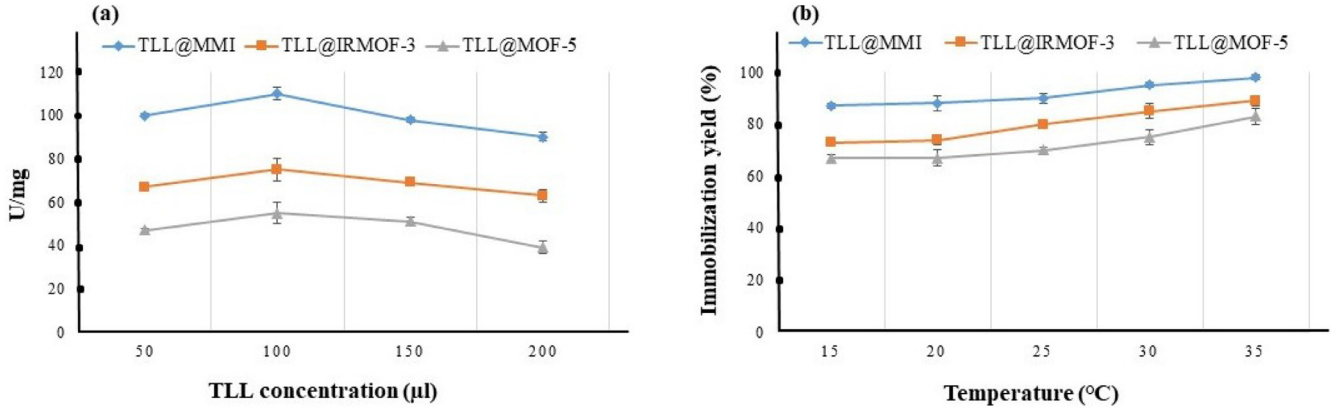

Fig. 6. Optimization of TLL@MOFs using a) different amounts of TLL and b) different temperatures to achieve the best immobilization yield.

also increased. This occurs because of excessive enzyme accumulation, which reduces enzyme activity. Therefore, 15–20 ˚C was chosen as the optimal temperature to immobilize the enzyme.

Next, 1.5 mg of TLL was immobilized on 10 mg of MOFs produced at 15–20 ˚C at 200 rpm for 24 h. With these parameters, immobilization yields of 67, 74, and 88% were obtained for TLL@MOF-5, TLL@IRMOF-3, and TLL@MMI, respectively. Moreover, specific activities of 47, 55, 110, and 75 U/mg were calculated for the free TLL, TLL@MOF-5, TLL@MMI, and TLL@IRMOF-3, respectively (Fig. 7).

3.3. Effect of NH_2

Various MOFs have been used to immobilize enzymes. MOFs with nitrogen atoms and amino groups, such as MIL-101-NH_2, PCN 333, and NH_2-MIL-53(Al), are popular for immobilizing enzymes [26,58–60]. Until now, no research group has paid attention to the fact that if the number of these amino groups changes, it affects enzyme immobilization and stability. Accordingly, we chose MOFs that have the same shape and surface area, and their holes are smaller than those of the enzyme; thus, we did not observe immobilization by another method.

Three MOFs containing different amounts of amino groups in their structures were chosen to immobilize TLL: MOF-5, IRMOF-3, and MMI. All ligands of IRMOF-3 have amino groups, half-ligands of MMI have amino groups, and MOF-5 does not have any amino groups.

Immobilization of the enzyme on MOF-5 resulted in TLL@MOF-5 being 1.17-fold more active than the free TLL (Fig. 7). TLL@IRMOF-3 was 1.6-fold more active than free TLL. While reducing the number of amino groups in the MOF structure(MMI), the immobilized TLL was 1.5-fold more active than the fully amino structure (IRMOF-3), which was used for immobilization. Therefore, although amino groups improve enzyme stability, the number of amino groups should also be considered.

To demonstrate the stability of the interaction between the enzyme and the MOF surface, a leaching test was performed. After 24 h of incubation, TLL@MOF-5, TLL@IRMOF-3, and TLL@MMI showed that 53%, 89%, and 74% of the enzyme remained on the substrate, respectively, and did not leach. This indicates the strength of the existing hydrogen

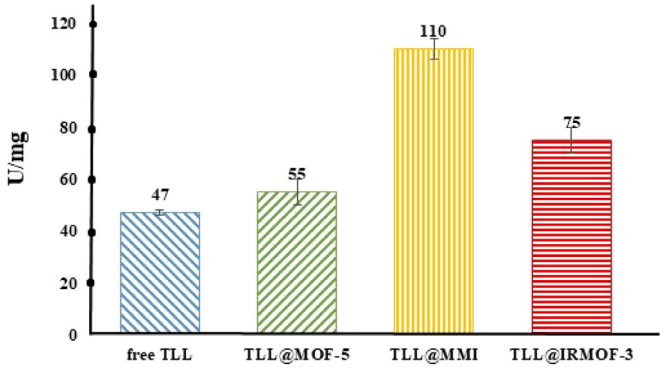

Fig. 7. Specific activity of free TLL, TLL@MOF-5, TLL@MMI, and TLL@IRMOF-3.

bond, which is due to the presence of the amino group. In MOF-5, which does not contain an amino group, the leaching percentage is higher, while in IRMOF-3, which contains a full amino group, the interaction between the enzyme and the surface of the MOF is highly stable.

Although TLL@IRMOF-3 showed a stable interaction between the enzyme and the MOF surface, the activity of the enzyme in that construct was lower than that of TLL@MMI. This result suggests that when the number of amino groups increases, excess hydrogen bonding probably leads to the destruction of the main structure of the enzyme, decreasing its activity.

3.4. Enzymatic properties of TLL@MOFs

3.4.1. Effect of pH on enzyme activity

The optimum pH values for TLL@MOF-5, TLL@MMI, and TLL@IRMOF-3 were investigated within the range of 6–10 at room temperature. As shown in Fig. 8b, although the optimum pH for free TLL was between 8 and 8.5, the three biocomposites showed an improved optimal pH within 8–10.

Furthermore, free TLL and the three biocomposites demonstrated different pH stabilities after incubation in buffers with different pH values (Fig. 8a). Free TLL did not show high stability between pH 6 and 7.5. However, the stability of TLL improved after immobilization; TLL@MMI showed excellent stability in the pH range of 6–10. Changes in the optimal pH and the stability of an enzyme at different pH values after immobilization have been reported previously [61,62].

3.4.2. Effect of solvent on enzyme activity

Solvents play an important role in chemical reactions [63]. Five common organic solvents that are generally used in synthetic reactions were investigated in this study to determine the stability of the synthesized biocomposites. Free TLL and the three biocomposites were incubated in a mixture of 20% and 50% (v/v) of each of the five solvents for 24 h (Fig. 9a, 9b). All biocomposites exhibited higher activities than the free enzyme, with TLL@MMI exhibiting the highest stability under all solvent conditions. After 24 h of incubation in a mixture of 50% (v/v) MeOH, TLL@MMI retained 80% of its activity, whereas TLL@MOF-5 and free TLL lost 50 and 60% of their activities, respectively.

3.4.3. Effect of temperature on enzyme activity

The thermal stability of the synthesized biocomposites was compared with that of free TLL (Fig. 10a). All three biocomposites exhibited higher activity after 2 h of incubation. Despite free TLL losing 60% activity at 75 ˚C, the TLL@MMI still showed 84% activity at the same temperature. Fig. 10b shows enzyme activity results after 24 h of incubation at 45 and 55 ˚C. The activity of all three biocomposites was greater than 97% within that temperature range, while free TLL lost 20% and 40% activity at 45 and 55 ˚C, respectively. TLL@MMI lost 50% of its activity at 45 and 55 ˚C after 95 and 72 h of incubation, respectively. Previous studies have reported that the immobilization of enzymes on MOFs improves their thermal stability [64,65].

3.4.4. Michaelis–Menten kinetic parameters

The Michaelis–Menten kinetic parameters of the reaction were measured to investigate the effects of immobilization on enzyme kinetics. The K_m (Michaelis constant) and V_{max} (maximum reaction velocity) were calculated by varying the *p*-NPB concentration. The V_{max} was 356.5, 302.3, 288.7, and 312.3 μmol/min for free TLL, TLL@MMI, TLL@IRMOF-3, and TLL@MOF-5, respectively. The K_m values were 1.032, 1.89, 2.01, and 1.63 μM for free TLL, TLL@MMI, TLL@IRMOF-3, and TLL@MOF-5, respectively. An increase in K_m indicates a lower affinity for the immobilized enzyme than for the free enzyme (substrate). This increase may be due to changes in the environment around the enzyme, restriction of substrate transfer to the active site, or a decrease in enzyme flexibility [66–68].

3.5. Thiazole synthesis

Because of the observed stability of the immobilized enzyme in different temperatures and organic solvents, we decided to use this biocomposite to synthesize organic compounds and measured its strength and ability in this field. In this study, the synthesis of thiazoles was investigated. In a recent study, we investigated the synthesis of pyrazoles using TLL@MMI [69].

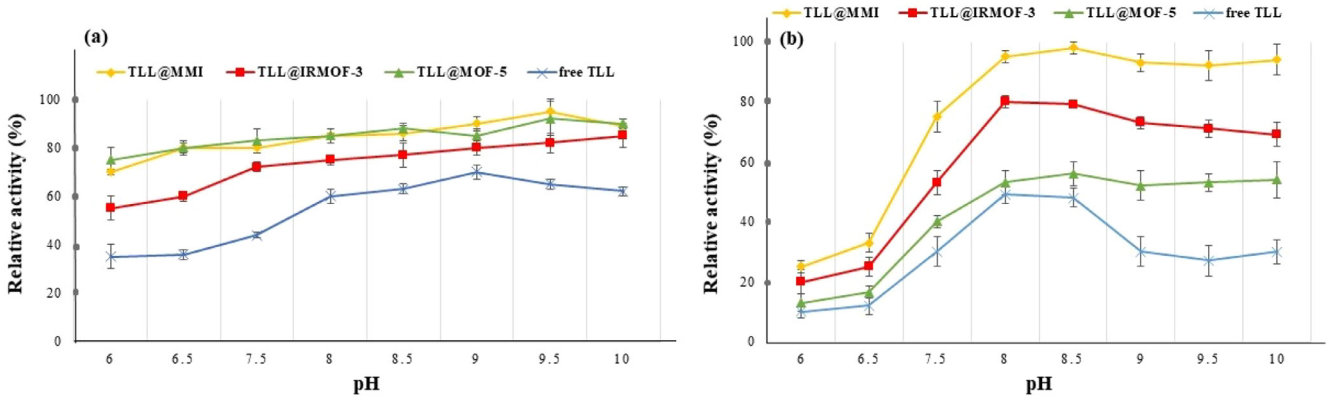

Fig. 8. pH stability and optimum pH for the activity of the MOF-immobilized enzymes. The experimental conditions were: a) 2 mg immobilized enzyme was dispersed in 20 ml of a 10 mM potassium phosphate buffer (pH 7.2) and incubated at different pH levels for 24 h; b) 2 mg immobilized enzyme in was dispersed in 20 ml of a 10 mM potassium phosphate buffer (pH 7.2), and enzyme activity was measured in different buffers (100% activity = 110 U/mg).

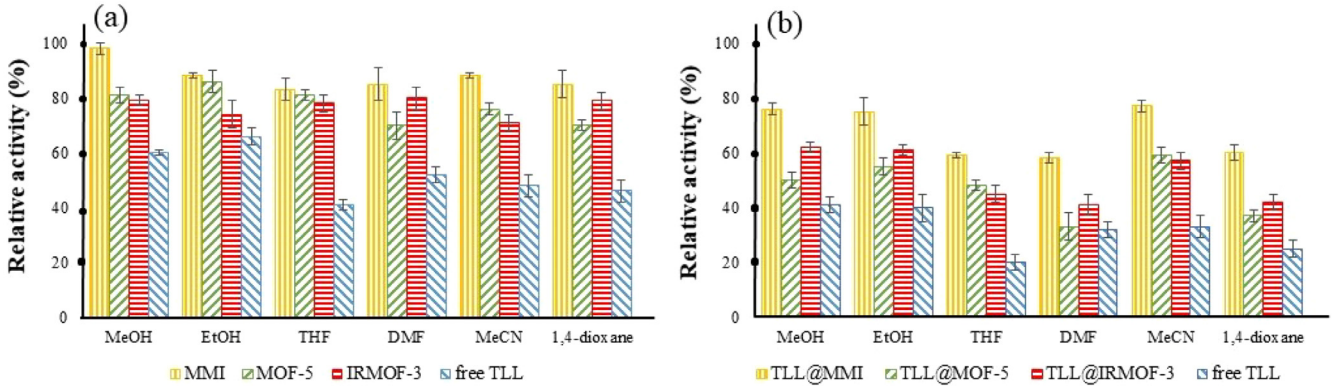

Fig. 9. a) Solvent stability of TLL@MOFs and free TLL in a) 20% v/v and b) 50% v/v organic solvents. Experimental conditions: 2 mg immobilized enzyme was dispersed in 20 ml of 10 mM potassium phosphate buffer (pH 7.2) and incubated for 24 h in different amounts of solvent (100% activity = 110 U/mg).

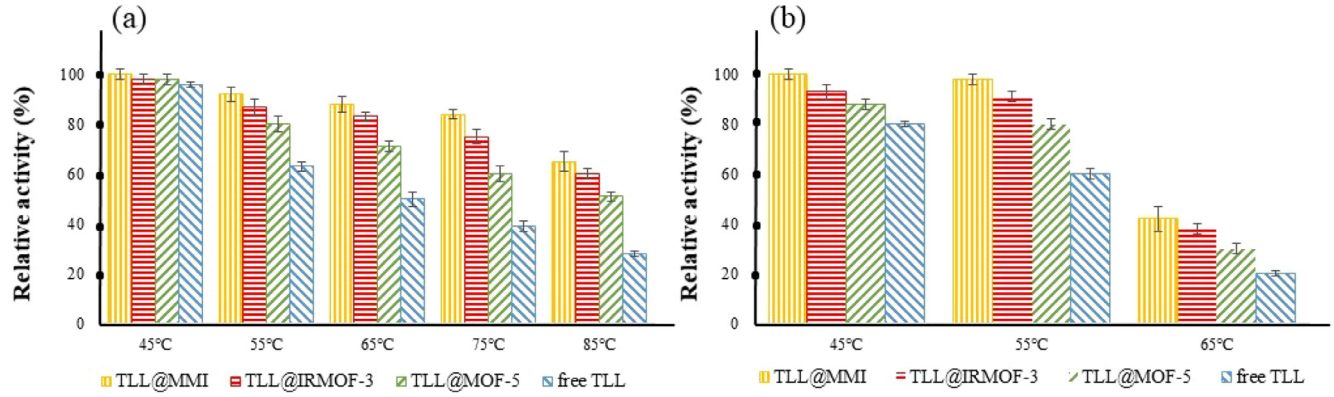

Fig. 10. Thermal stability of TLL@MOFs and free TLL after a) 2 h and b) 24 h of incubation at different temperatures. Experimental condition: 2 mg immobilized enzyme was dispersed in 20 ml of 10 mM potassium phosphate buffer (pH 7.2) and incubated for 2 and 24 h at different temperatures (100% activity = 110 U/mg).

Table 2
Optimization of (E)-4-(4-bromophenyl)-2-(2-(4-methoxybenzylidene) hydrazineyl) thiazole (4a) synthesis by adapting various parameters: solvent, temperature, and amount of catalyst.

Entry	Solvent	Temperature (°C)	Time (min)	mg of catalyst	Catalyst	Yield (%)
1	H_2O	45	90	5	TLL@MMI	87
2	Phosphate buffer (pH 9)	45	90	5	TLL@MMI	80
3	MeCN	45	90	5	TLL@MMI	51
4	DMF	45	90	5	TLL@MMI	72
5	EtOH	45	90	5	TLL@MMI	63
6	H_2O	45	30	10	TLL@MMI	92
7	H_2O	45	90	15	TLL@MMI	92
8	H_2O	45	90	10	TLL@MMI	98
9	H_2O	25	90	10	TLL@MMI	83
10	H_2O	45	90	10	MMI	31
11	H_2O	45	90	3	Free TLL	43
12	H_2O	45	90	-	-	Trace

Reagents and conditions: 4-methoxy benzaldehyde (1a) (5 mmol), 4-bromophenacyl bromide (2a) (5 mmol), thiosemicarbazide (3) (5 mmol), and solvent (10 mL).

Analogs of 2-arylidenehydrazinyl-4-arylthiozole exhibit antibacterial and antioxidant activities [70]. Because of their high bioactivity, several methods have been used to synthesize them [71,72]. Several previous studies about this are presented in Table 1. Most previous studies synthesized 2-arylidenehydrazinyl-4-arylthiozole analogs in two steps, which are time-consuming and require separate purification. In contrast, Reddy et al. [73] reported one-pot synthesis under green conditions using a metal catalyst.

In this study, we initially investigated the model reaction by mixing 4-methoxy benzaldehyde 1a (5 mmol), 4-bromophenacyl bromide 2a (5 mmol), and thiosemicarbazide 3 (5 mmol) at 45 °C in H_2O as a solvent and 5 mg of TLL@MMI as a catalyst. After 90 min, the yield was 87% (Table 2, entry 1). The model reaction was also tested at 45 °C with 5 mg of TLL@MMI in other solvents, such as phosphate buffer (pH 9) (table 2, entry 2), MeCN (table 2, entry 3), DMF (table 2, entry 4), and EtOH (table 2, entry 5). All the tested solvents exhibited lower reaction efficiencies than that of water. When the amount of catalyst was increased to 10 mg, the reaction yield reached 98% (Table 2, entry 8). However, using more than 15 mg of the catalyst was associated with decreased efficiency (Table 2, entry 7). Examining the model reaction at room temperature (25 °C) exhibited 83% yield at the optimal temperature of 45 °C. In addition, when the reaction was performed in the

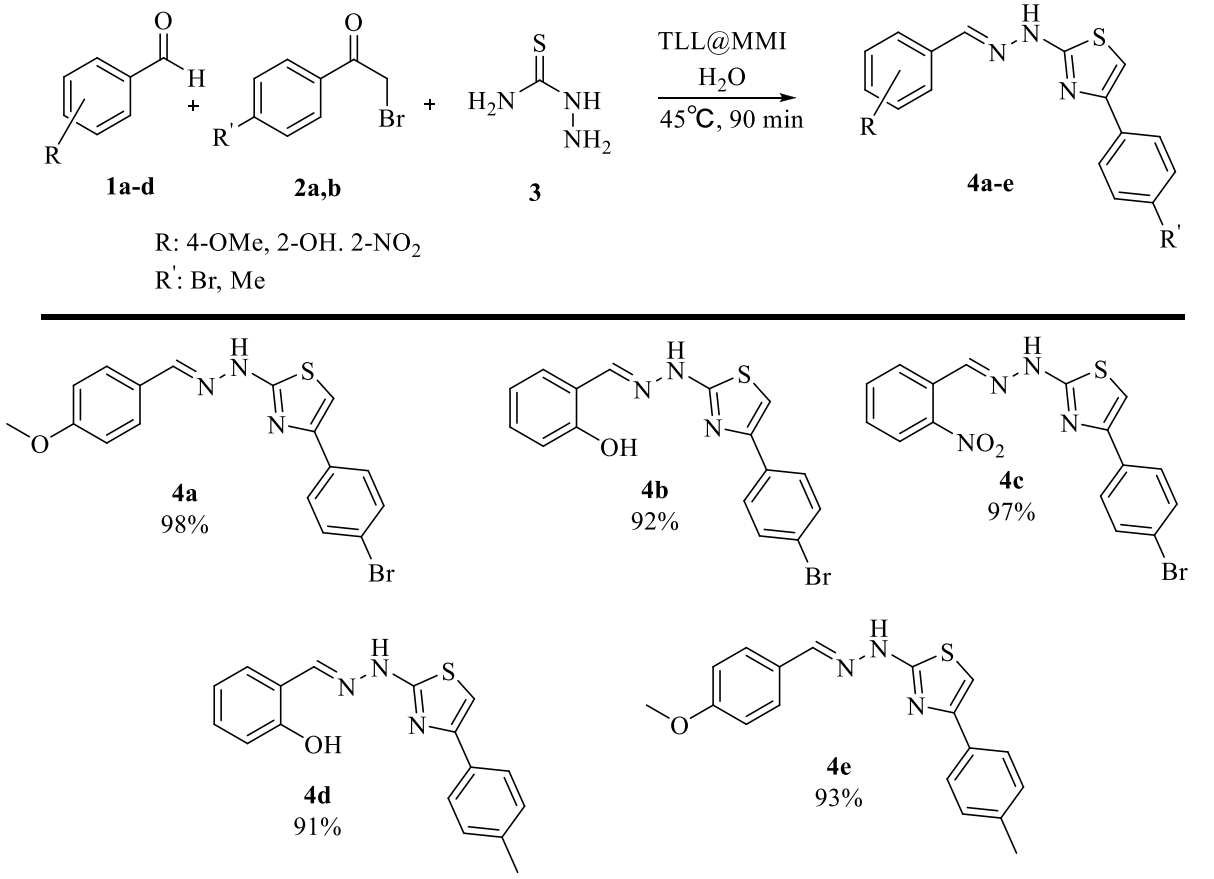

Scheme 1. TLL@MMI catalyzes the synthesis of 2-arylidenehydrazinyl-4-arylthiozole derivatives (4a–4e) in H_2O. Reagents and conditions: benzaldehydes (1a-1d) (5 mmol), phenacyl bromides (2a-2b) (5 mmol), thiosemicarbazide (3) (5 mmol), H_2O (10 mL), TLL@MMI catalyst (10 mg), 45°C.

absence of the enzyme (Table 2, entry 10), with a 31% yield. When the reaction was investigated in the absence of a catalyst, no product was observed (Table 2, entry 11).

To demonstrate the diversity of this reaction, derivatives with electron-donating and electron-accepting substituents were also selected (Scheme 1). All the derivatives were obtained with >90% yield. It is noteworthy that Reddy et al. achieved the same yield for 4a, but they used a larger amount of catalyst. Specifically, they coated Cu nanoparticles onto TiO_2, yielding 25 mg of CuONPs/TiO_2-synthesized thiazole for each 5 mmol of substrate.

3.6. Reusability

The catalysts used in the reactions were separated, washed, and dried for reuse. Subsequently, the activity of the recovered catalysts was measured before the next use. After six cycles, the catalysts retained 87% of their activity (Fig. 11). The high stability and reusability of the catalysts we generated indicate that they can be used for various chemical reactions under different conditions.

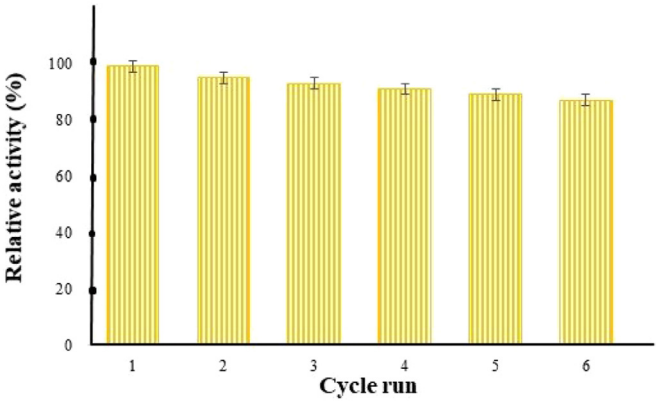

Fig. 11. Reusability of the TLL@MMI catalyst for the thiazole synthesis reaction.

4. Conclusion

In this study, we produced three new biocomposites by changing the number of amino groups in MOF structures and immobilizing TLL in them through surface adsorption: TLL@MOF-5, TLL@IRMOF-3, and TLL@MMI. TLL@MMI was more effective than the other MOFs, showing the highest stability and chemical reaction efficiency. This information indicates that increasing the number of amine groups in the structure of the MOF up to a certain amount has a positive effect on enzyme activity and stability; however, a higher number of amine groups over this limit causes negative effects [77].

5. Experimental

(E)-4-(4-bromophenyl)-2-(2-(4-methoxybenzylidene) hydrazineyl) thiazole (4a). ^{1}H NMR (300 MHz, DMSO-d_6) 8.00 (s, 1H), 7.80 (d, J = 8.2 Hz, 2H), 7.66 – 7.55 (m, 4H), 7.39 (s, 1H), 7.01 (d, J = 8.3

Hz, 2H), 3.80 (s, 3H).^{13}C NMR (75 MHz, DMSO-d_6) δ 173.68, 165.56, 153.85, 147.21, 138.72, 136.76, 133.14, 132.80, 132.04, 125.85, 119.57, 109.59, 60.49.

(E)-2-((2-(4-(4-bromophenyl) thiazol-2-yl) hydrazineylidene) methyl) phenol (4b). ^{1}H NMR (300 MHz, DMSO-d_6) δ 12.22 (s, 1H), 10.12 (s, 1H), 8.03 (s, 1H), 7.80 (d, J = 8.3 Hz, 2H), 7.67 – 7.55 (m, 3H), 7.40 (s, 1H), 7.22 (t, J = 7.6 Hz, 1H), 7.01-6.79 (m, 2H).

(E)-4-(4-bromophenyl)-2-(2-(2-nitrobenzylidene) hydrazineyl) thiazole (4c). ^{1}H NMR (300 MHz, DMSO-d_6) δ 12.60 (s, 1H), 8.43 (s, 1H), 8.09 – 7.96 (m, 3H), 7.87 – 7.73 (m, 3H), 7.61 (d, J = 7.5 Hz, 2H), 7.47 (s, 1H).

(E)-2-((2-(4-(p-tolyl) thiazol-2-yl) hydrazineylidene) methyl) phenol (4d). ^{1}H NMR (300 MHz, DMSO-d_6) δ 10.15 (s, 1H), 8.33 (s, 1H), 7.63 (d, J = 8.1 Hz, 2H), 7.53 – 7.14 (m, 4H), 7.00 – 6.75 (m, 3H), 2.4 (s, 3H).

(E)-2-(2-(4-methoxybenzylidene) hydrazineyl)-4-(p-tolyl) thiazole (4e). ^{1}H NMR (300 MHz, DMSO-d_6) δ 7.98 (s, 1H), 7.86 (d, J = 7.7 Hz, 2H), 7.59 (d, J = 8.2 Hz, 2H), 7.33 – 7.18 (m, 3H), 7.03 – 6.97 (m, 2H), 3.80 (s, 3H), 2.4 (s, 3H).

Declaration of competing interest

There are no declarations of interest.

CRediT authorship contribution statement

Zeynab Rangraz: Writing – original draft, Visualization, Validation, Methodology, Investigation, Formal analysis, Conceptualization. **Mostafa M. Amini:** Writing – review & editing, Validation, Data curation. **Zohreh Habibi:** Writing – review & editing, Supervision, Project administration, Funding acquisition.

Acknowledgements

This research was financially supported by Shahid Beheshti University of Tehran which the authors are thankful.

References

[1] J. Cui, Y. Zhao, R. Liu, C. Zhong, S. Jia, Surfactant-activated lipase hybrid nanoflowers with enhanced enzymatic performance, Sci. Rep. 6 (2016) 27928.
[2] Z. Wang, R. Wang, Z. Geng, X. Luo, J. Jia, S. Pang, X. Fan, M. Bilal, J. Cui, Enzyme hybrid nanoflowers and enzyme@ metal–organic frameworks composites: fascinating hybrid nanobiocatalysts, Crit. Rev. Biotechnol. 44 (2024) 674–697.
[3] J. Cui, Y. Feng, S. Jia, Silica encapsulated catalase@ metal-organic framework composite: A highly stable and recyclable biocatalyst, Chemical Engineering Journal 351 (2018) 506–514.
[4] J. Cui, S. Ren, T. Lin, Y. Feng, S. Jia, Shielding effects of Fe3+-tannic acid nanocoatings for immobilized enzyme on magnetic Fe3O4@ silica core shell nanosphere, Chemical Engineering Journal 343 (2018) 629–637.
[5] J. Cui, L. Cui, S. Jia, Z. Su, S. Zhang, Hybrid cross-linked lipase aggregates with magnetic nanoparticles: a robust and recyclable biocatalysis for the epoxidation of oleic acid, J. Agric. Food Chem. 64 (2016) 7179–7187.
[6] X. Shen, Y. Du, Z. Du, X. Tang, P. Li, J. Cheng, R. Yan, J. Cui, Construction of enzyme@ glutathione hybrid metal-organic frameworks: glutathione-boosted microenvironment fine-tuning of biomimetic immobilization for improving catalytic performance, Mater. Today Chem. 27 (2023) 101326.
[7] J. Cui, X. Tang, Q. Ma, Y. Chang, Q. Zhang, S. Jia, Cross-linked α-amylase aggregates on Fe3O4 magnetic nanoparticles modified with polydopamine/polyethyleneimine for efficient hydrolysis of starch, Particuology 90 (2024) 98–105.
[8] P. Li, J. Jia, Z. Geng, S. Pang, R. Wang, M. Bilal, H. Bian, J. Cui, S. Jia, A dual enzyme-phosphate hybrid nanoflower for glutamate detection, Particuology 83 (2023) 63–70.
[9] Y. Feng, Y. Du, G. Kuang, L. Zhong, H. Hu, S. Jia, J. Cui, Hierarchical micro-and mesoporous ZIF-8 with core–shell superstructures using colloidal metal sulfates as soft templates for enzyme immobilization, J. Colloid. Interface Sci. 610 (2022) 709–718.
[10] F.A.P. Lage, J.J. Bassi, M.C.C. Corradini, L.M. Todero, J.H.H. Luiz, A.A. Mendes, Preparation of a biocatalyst via physical adsorption of lipase from Thermomyces lanuginosus on hydrophobic support to catalyze biolubricant synthesis by esterification reaction in a solvent-free system, Enzyme Microb. Technol. 84 (2016) 56–67.
[11] O. Gherbovet, F. Ferreira, A. Clément, M. Ragon, J. Durand, S. Bozonnet, M.J. O'Donohue, R. Fauré, Regioselective chemoenzymatic syntheses of ferulate conjugates as chromogenic substrates for feruloyl esterases, Beilstein. J. Org. Chem. 17 (2021) 325–333.
[12] E. Abreu Silveira, S. Moreno-Perez, A. Basso, S. Serban, R. Pestana-Mamede, P.W. Tardioli, C.S. Farinas, N. Castejon, G. Fernandez-Lorente, J. Rocha-Martin, J.M. Guisan, Biocatalyst engineering of Thermomyces Lanuginosus lipase adsorbed on hydrophobic supports: Modulation of enzyme properties for ethanolysis of oil in solvent-free systems, J. Biotechnol. 289 (2019) 126–134.
[13] G.D. Yadav, I.V. Borkar, Lipase-catalyzed hydrazinolysis of phenyl benzoate: Kinetic modeling approach, Process Biochemistry 45 (2010) 586–592.
[14] Y. Yücel, Optimization of immobilization conditions of Thermomyces lanuginosus lipase on olive pomace powder using response surface methodology, Biocatal. Agric. Biotechnol. 1 (2012) 39–44.
[15] A.L.S. Coelho, R.C. Orlandelli, Immobilized microbial lipases in the food industry: a systematic literature review, Crit. Rev. Food Sci. Nutr. 61 (2021) 1689–1703.
[16] F. Rafiee, M. Rezaee, Different strategies for the lipase immobilization on the chitosan based supports and their applications, Int. J. Biol. Macromol. 179 (2021) 170–195.
[17] J. Zhang, X. Chen, P. Lv, W. Luo, Z. Wang, J. Xu, Z. Wang, Bionic-immobilized recombinant lipase obtained via bio-silicification and its catalytic performance in biodiesel production, Fuel 304 (2021) 121594.
[18] K. Dopierała, A. Kołodziejczak-Radzimska, K. Prochaska, T. Jesionowski, Immobilization of lipase in Langmuir – Blogett film of cubic silsesquioxane on the surface of zirconium dioxide, Appl. Surf. Sci. 573 (2022) 151184.
[19] X. Lian, Y. Fang, E. Joseph, Q. Wang, J. Li, S. Banerjee, C. Lollar, X. Wang, H.C. Zhou, Enzyme–MOF (metal–organic framework) composites, Chem. Soc. Rev. 46 (2017) 3386–3401.
[20] M.G. Pereira, F.D.A. Facchini, A.M. Polizeli, A.C. Vici, J.A. Jorge, B.C. Pessela, G. Fernandez-Lorente, J.M. Guisán, M.d.L.T. de Moraes Polizeli, Stabilization of the lipase of Hypocrea pseudokoningii by multipoint covalent immobilization after chemical modification and application of the biocatalyst in oil hydrolysis, Journal of Molecular Catalysis B: Enzymatic 121 (2015) 82–89.
[21] H. Li, Y. Sun, Y. Li, J. Du, Alkaline phosphatase activity assay with luminescent metal organic frameworks-based chemiluminescent resonance energy transfer platform, Microchemical Journal 160 (2021) 105665.
[22] Y.J. Lee, Y.J. Chang, D.J. Lee, J.P. Hsu, Water stable metal-organic framework as adsorbent from aqueous solution: A mini-review, J. Taiwan. Inst. Chem. Eng. 93 (2018) 176–183.
[23] L. Zhong, Y. Feng, H. Hu, J. Xu, Z. Wang, Y. Du, J. Cui, S. Jia, Enhanced enzymatic performance of immobilized lipase on metal organic frameworks with superhydrophobic coating for biodiesel production, J. Colloid. Interface Sci. 602 (2021) 426–436.
[24] S. Liang, X.L. Wu, J. Xiong, M.H. Zong, W.Y. Lou, Metal-organic frameworks as novel matrices for efficient enzyme immobilization: An update review, Coord. Chem. Rev. 406 (2020) 213149.
[25] A.R.M. Silva, J.Y.N.H. Alexandre, J.E.S. Souza, J.G.L. Neto, P.G. de Sousa Júnior, M.V.P. Rocha, J.C.S. dos Santos, The Chemistry and Applications of Metal–Organic Frameworks (MOFs) as Industrial Enzyme Immobilization Systems, Molecules. (2022).
[26] W. Liang, P. Wied, F. Carraro, C.J. Sumby, B. Nidetzky, C.K. Tsung, P. Falcaro, C.J. Doonan, Metal–organic framework-based enzyme biocomposites, Chem. Rev. 121 (2021) 1077–1129.
[27] J. Zhang, Z. Wang, W. Zhuang, H. Rabiee, C. Zhu, J. Deng, L. Ge, H. Ying, Amphiphilic Nanointerface: Inducing the Interfacial Activation for Lipase, ACS. Appl. Mater. Interfaces. 14 (2022) 39622–39636.
[28] R.C. Rodrigues, J.J. Virgen-Ortíz, J.C.S. dos Santos, Á. Berenguer-Murcia, A.R. Alcantara, O. Barbosa, C. Ortiz, R. Fernandez-Lafuente, Immobilization of lipases on hydrophobic supports: immobilization mechanism, advantages, problems, and solutions, Biotechnol. Adv. 37 (2019) 746–770.
[29] J.M. Palomo, G. Muñoz, G. Fernández-Lorente, C. Mateo, R. Fernández-Lafuente, J.M. Guisán, Interfacial adsorption of lipases on very hydrophobic support (octadecyl–Sepabeads): immobilization, hyperactivation and stabilization of the open form of lipases, Journal of Molecular Catalysis B: Enzymatic 19-20 (2002) 279–286.
[30] L. Zhong, Z. Wang, X. Ye, J. Cui, Z. Wang, S. Jia, Molecular simulations guide immobilization of lipase on nest-like ZIFs with regulatable hydrophilic/hydrophobic surface, J. Colloid. Interface Sci. 667 (2024) 199–211.
[31] J.M.F. Silva, K.P. dos Santos, E.S. dos Santos, N.S. Rios, L.R.B. Gonçalves, Immobilization of Thermomyces lanuginosus lipase on a new hydrophobic support (Streamline phenyl™): Strategies to improve stability and reusability, Enzyme Microb. Technol. 163 (2023) 110166.
[32] S. Kouser, A. Hezam, M.J.N. Khadri, S.A. Khanum, A review on zeolite imidazole frameworks: synthesis, properties, and applications, Journal of Porous Materials 29 (2022) 663–681.
[33] M.R.S. Moguei, Z. Habibi, M. Shahedi, M. Yousefi, A. Alimoradi, S. Mobini, M. Mohammadi, Immobilization of Thermomyces lanuginosus lipase through isocyanide-based multi component reaction on multi-walled carbon nanotube: application for kinetic resolution of rac-ibuprofen, Biotechnology Reports 35 (2022) e00759.
[34] S.H. Ali, A.R. Sayed, Review of the synthesis and biological activity of thiazoles, Synth. Commun. 51 (2021) 670–700.
[35] Z.X. Niu, Y.T. Wang, S.N. Zhang, Y. Li, X.B. Chen, S.Q. Wang, H.M. Liu, Application and synthesis of thiazole ring in clinically approved drugs, Eur. J. Med. Chem. 250 (2023) 115172.
[36] B. Gu, Z.E Hu, Z.J. Yang, J. Li, Z.W. Zhou, N. Wang, X.Q. Yu, Probing the Mechanism of CAL-B-Catalyzed aza-Michael Addition of Aniline Compounds with Acrylates Using Mutation and Molecular Docking Simulations, ChemistrySelect. 4 (2019) 3848–3854.
[37] J. Priego, C. Ortíz-Nava, M. Carrillo-Morales, A. López-Munguía, J. Escalante, E. Castillo, Solvent engineering: an effective tool to direct chemos-

electivity in a lipase-catalyzed Michael addition, Tetrahedron. 65 (2009) 536–539.
[38] B.H. Xie, Z. Guan, Y.H. He, Promiscuous enzyme-catalyzed Michael addition: synthesis of warfarin and derivatives, Journal of Chemical Technology & Biotechnology 87 (2012) 1709–1714.
[39] K. Li, T. He, C. Li, X.W. Feng, N. Wang, X.Q. Yu, Lipase-catalysed direct Mannich reaction in water: utilization of biocatalytic promiscuity for C–C bond formation in a "one-pot" synthesis, Green Chemistry 11 (2009) 777–779.
[40] S. Kłossowski, B. Wiraszka, S. Berłożecki, R. Ostaszewski, Model Studies on the First Enzyme-Catalyzed Ugi Reaction, Org. Lett. 15 (2013) 566–569.
[41] B. Arora, P.S. Pandey, M.N. Gupta, Lipase catalyzed Cannizzaro-type reaction with substituted benzaldehydes in water, Tetrahedron. Lett. 55 (2014) 3920–3922.
[42] X. Tian, S. Zhang, L. Zheng, First Novozym 435 lipase-catalyzed Morita–Baylis–Hillman reaction in the presence of amides, Enzyme Microb. Technol. 84 (2016) 32–40.
[43] B.P. Dwivedee, S. Soni, M. Sharma, J. Bhaumik, J.K. Laha, U.C. Banerjee, Promiscuity of Lipase-Catalyzed Reactions for Organic Synthesis: A Recent Update, ChemistrySelect. 3 (2018) 2441–2466.
[44] J. Hafizovic, M. Bjørgen, U. Olsbye, P.D.C. Dietzel, S. Bordiga, C. Prestipino, C. Lamberti, K.P. Lillerud, The Inconsistency in Adsorption Properties and Powder XRD Data of MOF-5 Is Rationalized by Framework Interpenetration and the Presence of Organic and Inorganic Species in the Nanocavities, J. Am. Chem. Soc. 129 (2007) 3612–3620.
[45] H. Deng, C.J. Doonan, H. Furukawa, R.B. Ferreira, J. Towne, C.B. Knobler, B. Wang, O.M. Yaghi, Multiple Functional Groups of Varying Ratios in Metal-Organic Frameworks, Science (1979) 327 (2010) 846–850.
[46] J. Li, Y. Wang, Y. Yu, Q. Li, Functionality proportion and corresponding stability study of multivariate metal-organic frameworks, Chinese Chemical Letters 29 (2018) 837–841.
[47] R.E. Pemta Tia Deka, and Didik Prasetyoko Crystal Growth of IRMOF-3
[48] (Isoreticular Metal-Organic Frameworks-3) Synthesized using Solvothermal Method, IPTEK, Journal of Proceeding Series 1 (2014).
[49] M.M. Bradford, A rapid and sensitive method for the quantitation of microgram quantities of protein utilizing the principle of protein-dye binding, Anal. Biochem. 72 (1976) 248–254.
[50] J. Boudrant, J.M. Woodley, R. Fernandez-Lafuente, Parameters necessary to define an immobilized enzyme preparation, Process Biochemistry 90 (2020) 66–80.
[51] T. Roodbar Shojaei, S. Soltani, M. Derakhshani, Chapter 6 - Synthesis, properties, and biomedical applications of inorganic bionanomaterials, Fundamentals of Bionanomaterials (2022) 139–174 Elsevier.
[52] P. Sharma, R. Sharma, R. Mukhiya, K. Awasthi, M. Kumar, 16 - Zinc-Oxide based EGFET pH sensors, in: K. Awasthi (Ed.), Nanostructured Zinc Oxide, Elsevier, 2021, pp. 459–481.
[53] M.B. Binish, P. Binu, V.G. Gopikrishna, M. Mohan, Chapter 15 - Potential of anaerobic bacteria in bioremediation of metal-contaminated marine and estuarine environment, Microbial Biodegradation and Bioremediation (2022) 305–326 (Second Edition), Elsevier.
[54] R. Sabouni, H. Kazemian, S. Rohani, A novel combined manufacturing technique for rapid production of IRMOF-1 using ultrasound and microwave energies, Chemical Engineering Journal 165 (2010) 966–973.
[55] A. Martinez-Felipe, A.G. Cook, J.P. Abberley, R. Walker, J.M. Storey, C.T. Imrie, An FT-IR spectroscopic study of the role of hydrogen bonding in the formation of liquid crystallinity for mixtures containing bipyridines and 4-pentoxybenzoic acid, RSC. Adv. 6 (2016) 108164–108179.
[56] D. Zhao, Y. Deng, D. Han, L. Tan, Y. Ding, Z. Zhou, H. Xu, Y. Guo, Exploring structural variations of hydrogen-bonding patterns in cellulose during mechanical pulp refining of tobacco stems, Carbohydr. Polym. 204 (2019) 247–254.
[57] J. Gomes, J. Batra, V.R. Chopda, P. Kathiresan, A.S. Rathore, Chapter 25 - Monitoring and Control of Bioethanol Production From Lignocellulosic Biomass, Waste Biorefinery (2018) 727–749 Elsevier.
[58] M. Nasrollahzadeh, M. Atarod, M. Sajjadi, S.M. Sajadi, Z. Issaabadi, Chapter 6 - Plant-Mediated Green Synthesis of Nanostructures: Mechanisms, Characterization, and Applications, in: M. Nasrollahzadeh, S.M. Sajadi, M. Sajjadi, Z. Issaabadi, M. Atarod (Eds.), Interface Science and Technology, Elsevier, 2019, pp. 199–322.
[59] C. Doonan, R. Riccò, K. Liang, D. Bradshaw, P. Falcaro, Metal–Organic Frameworks at the Biointerface: Synthetic Strategies and Applications, Acc. Chem. Res. 50 (2017) 1423–1432.
[60] R. Singh, M. Musameh, Y. Gao, B. Ozcelik, X. Mulet, C.M. Doherty, Stable MOF@ enzyme composites for electrochemical biosensing devices, Journal of Materials Chemistry C 9 (2021) 7677–7688.
[61] M.A. Molina, J. Díez-Jaén, M. Sánchez-Sánchez, R.M. Blanco, One-pot laccase@MOF biocatalysts efficiently remove bisphenol A from water, Catal. Today 390-391 (2022) 265–271.
[62] J. Peng, E. Wu, X. Lou, Q. Deng, X. Hou, C. Lv, Q. Hu, Anthraquinone removal by a metal-organic framework/polyvinyl alcohol cryogel-immobilized laccase: Effect and mechanism exploration, Chemical Engineering Journal 418 (2021) 129473.
[63] M. Ashjari, M. Garmroodi, F. Ahrari, M. Yousefi, M. Mohammadi, Soluble enzyme cross-linking via multi-component reactions: a new generation of cross-linked enzymes, Chemical Communications 56 (2020) 9683–9686.
[64] N.R. Candeias, B. Assoah, S.P. Simeonov, Production and synthetic modifications of shikimic acid, Chem. Rev. 118 (2018) 10458–10550.
[65] M. Ashjari, M. Mohammadi, R. Badri, Chemical amination of Rhizopus oryzae lipase for multipoint covalent immobilization on epoxy-functionalized supports: Modulation of stability and selectivity, Journal of Molecular Catalysis B: Enzymatic 115 (2015) 128–134.
[66] W. Liang, H. Xu, F. Carraro, N.K. Maddigan, Q. Li, S.G. Bell, D.M. Huang, A. Tarzia, M.B. Solomon, H. Amenitsch, Enhanced activity of enzymes encapsulated in hydrophilic metal–organic frameworks, J. Am. Chem. Soc. 141 (2019) 2348–2355.
[67] F. Lyu, Y. Zhang, R.N. Zare, J. Ge, Z. Liu, One-pot synthesis of protein-embedded metal–organic frameworks with enhanced biological activities, Nano Lett. 14 (2014) 5761–5765.
[68] S.S. Nadar, V.K. Rathod, Sonochemical effect on activity and conformation of commercial lipases, Appl. Biochem. Biotechnol. 181 (2017) 1435–1453.
[69] S.S. Nadar, V.K. Rathod, Immobilization of proline activated lipase within metal organic framework (MOF), Int. J. Biol. Macromol. 152 (2020) 1108–1112.
[70] Z. Rangraz, M.M. Amini, Z. Habibi, One-Pot Synthesis of 1,3,5-Trisubstitued Pyrazoles via Immobilized Thermomyces lanuginosus Lipase (TLL) on a Metal–Organic Framework, ACS. Omega 9 (2024) 19089–19098.
[71] M.S. Alam, J.U. Ahmed, D.U. Lee, Synthesis, antibacterial, antioxidant activity and QSAR studies of novel 2-arylidenehydrazinyl-4-arylthiazole analogues, Chemical and Pharmaceutical Bulletin 62 (2014) 1259–1268.
[72] Q. Ding, D. Zhu, H. Jin, J. Chen, J. Ding, H. Wu, Eco-Friendly one-pot synthesis of 2, 4-disubstituted thiazoles by grinding under catalyst-and solvent-free conditions, Phosphorus, Sulfur, and Silicon 186 (2011) 220–224.
[73] L. Lohrey, T.N. Uehara, S. Tani, J. Yamaguchi, H.U. Humpf, K. Itami, 2, 4-and 2, 5-Disubstituted Arylthiazoles: Rapid Synthesis by C–H Coupling and Biological Evaluation, European. J. Org. Chem. 2014 (2014) 3387–3394.
[74] G.T. Reddy, G. Kumar, N.G. Reddy, Water-Mediated One-pot Three-Component Synthesis of Hydrazinyl-Thiazoles Catalyzed by Copper Oxide Nanoparticles Dispersed on Titanium Dioxide Support: A Green Catalytic Process, Adv. Synth. Catal. 360 (2018) 995–1006.
[75] S. Bharti, G. Nath, R. Tilak, S. Singh, Synthesis, anti-bacterial and anti-fungal activities of some novel Schiff bases containing 2, 4-disubstituted thiazole ring, Eur. J. Med. Chem. 45 (2010) 651–660.
[76] H. Nagarajaiah, A.K. Mishra, J.N. Moorthy, Mechanochemical solid-state synthesis of 2-aminothiazoles, quinoxalines and benzoylbenzofurans from ketones by one-pot sequential acid-and base-mediated reactions, Org. Biomol. Chem. 14 (2016) 4129–4135.
[77] E.S. Ramadan, Synthesis of Biologically Active [4-(4-Bromophenyl)-2-thiazolyl] hydrazones and their D-Galactose Derivatives, Chin. J. Chem. 28 (2010) 594–600.